# Cross-Coupling Between Longitudinal and Lateral Aircraft Dynamics in a Spiral Dive

M. Velger* and J. Shinar†
*Technion—Israel Institute of Technology, Haifa, Israel*

**In this paper, the spiral dive phenomenon, encountered mainly in light, unswept wing, general aviation aircraft, is investigated. The investigation was performed by a nonlinear five-degrees-of-freedom simulation of the aircraft response to elevator deflection during a gliding turn. The simulation results indicate that this phenomenon is generated by an aerodynamic cross-coupling created owing to the dependence of the rolling moment coefficient on the angle of attack. The paper presents the mechanism of the development of the phenomenon, which is composed of three motions at almost separate time scales: a fast longitudinal motion, a slowly divergent lateral motion, and a combined kinematic response of the aircraft. A criterion for "recovery by elevator only" from spiral dive is defined and flight conditions for failure of successful recovery are determined. Results show that recovery becomes more difficult for steeper glides, larger bank angles, and lower velocities.**

## Nomenclature

| | |
|---|---|
| $b$ | = wing span |
| $\bar{c}$ | = mean aerodynamic chord |
| $C_l$ | = rolling moment coefficient |
| $C_m$ | = pitching moment coefficient |
| $C_n$ | = yawing moment coefficient |
| $C_L$ | = lift coefficient |
| $C_y$ | = side force coefficient |
| $g$ | = acceleration of gravity = 9.81 m/s$^2$ |
| $I_x, I_y, I_z$ | = moments of inertia about principal axes |
| $m$ | = aircraft mass |
| $p$ | = roll rate |
| $q$ | = pitch rate |
| $r$ | = yaw rate |
| $q_\infty$ | = dynamic pressure = $\frac{1}{2}\rho V^2$ |
| $S$ | = wing area |
| $V$ | = aircraft velocity |
| $\alpha$ | = angle of attack |
| $\beta$ | = sideslip angle |
| $\gamma$ | = flight-path angle |
| $\delta_e, \delta_r, \delta_a$ | = elevator, rudder, and aileron deflections, respectively |
| $\rho$ | = air density |
| $\theta$ | = pitch attitude |
| $\phi$ | = bank angle |

## I. Introduction

THE phenomenon of spiral dive has been known to pilots of light, general aviation aircraft for many years. It occurs in a gliding turn when the pilot tries to stop the descent by using the elevator only. Experience has shown that in some flight conditions the turn becomes tighter, the glide angle increasing and not decreasing as desired. The recovery from a spiral dive is rather simple: wings have to be leveled before the use of the elevator.

Although the existence of the spiral dive, as well as the recovery from it, has been of common pilot knowledge, it has not received a clear explanation either in pilot handbooks or in the scientific literature. The well-known "Jeppesen Private Pilot Course"[1] warns noninstrument rated pilots with regard to this phenomenon:

> A very serious, but common type of sensory illusion may occur when a noninstrument rated pilot continues flight into instrument conditions. When the pilot loses outside visual reference, the aircraft may enter a very slight bank at a rate undetectable to the sense of balance. This bank will generally increase until there is a noticeable loss of altitude. Noting the decrease in altitude, and still assuming level flight, the pilot may pull back on the wheel and perhaps add power in an attempt to regain the lost altitude. This maneuver only serves to tighten the spiral, unless the bank attitude of the aircraft is corrected first.

The origin of this phenomenon is the dynamic and aerodynamic cross-coupling which exists between longitudinal and lateral aircraft dynamics in every not entirely symmetrical flight condition.

In the last decades, a considerable research effort has been conducted to analyze the longitudinal/lateral cross-coupling in aircraft dynamics. Attention has been focused on phenomena associated with rapid roll rates and high angles of attack such as inertial cross-coupling,[2-8] "jump" phenomena,[9,10] and degradation stability in highly nonsymmetrical flight.[11-15]

In this paper a cross-coupling occurring at relatively small angles of attack and at almost negligible roll rate is analyzed.

In Sec. II the five-degrees-of-freedom mathematical model and the equilibrium gliding turn values, which are used as initial conditions in solving the nonlinear equations of motion, are presented. In Sec. III a qualitative explanation of the spiral dive, based on the full simulation of the phenomenon, is given. In Sec. IV a criterion for "recovery by elevator only" is proposed and the flight conditions for successful recovery are shown. In Sec. V an attempt is made to describe the phenomenon with linearized equations of motion. Aircraft data are presented in Appendix A and the stability derivatives definitions in Appendix B.

## II. Mathematical Model

The analysis is based on the results of a nonlinear five-degrees-of-freedom (constant speed) digital simulation of aircraft response to elevator inputs in a steady-state gliding turn.

The angle of attack differential equation is written in wind axes. The lateral translational equation as well as the rotational degrees-of-freedom equations are written in principal body axes. Simplifying assumptions are 1) constant speed, 2) constant air density, 3) linear aerodynamics, and 4) negligible thrust component in the direction of the lift compared to the lift.

Received Aug. 10, 1981; revision received March 8, 1982. 

*Graduate Student, Department of Aeronautical Engineering.
†Associate Professor, Department of Aeronautical Engineering.

The nonlinear equations of motion used in the computations of time histories are

$$\dot{\alpha}=q+\left[\left(\frac{g}{V}\sin\theta-r\sin\beta\right)\sin\alpha+\left(\frac{g}{V}\cos\theta\cos\phi-p\sin\beta\right)\cos\alpha-\frac{q_\infty S}{mV}C_L\right]\frac{1}{\cos\beta} \quad (1)$$

$$\dot{\beta}=p\sin\alpha-r\cos\alpha+\left[\frac{q_\infty S}{mV}C_y+\frac{g}{V}\cos\theta\sin\phi\right]\frac{1}{\cos\beta} \quad (2)$$

$$\dot{p}=\frac{I_y-I_z}{I_x}qr+\frac{q_\infty Sb}{I_x}C_l \quad (3)$$

$$\dot{q}=\frac{I_z-I_x}{I_y}pr+\frac{q_\infty S\bar{c}}{I_y}C_m \quad (4)$$

$$\dot{r}=\frac{I_x-I_y}{I_z}pq+\frac{q_\infty Sb}{I_z}C_n \quad (5)$$

$$\dot{\phi}=p+q\tan\theta\sin\phi+r\tan\theta\cos\phi \quad (6)$$

$$\dot{\theta}=q\cos\phi-r\sin\phi \quad (7)$$

The flight-path angle is described by

$$\sin\gamma=\sin\theta\cos\beta\cos\alpha-\sin\phi\cos\theta\sin\beta-\cos\phi\cos\theta\cos\beta\sin\alpha \quad (8)$$

This angle is measured between the velocity vector component in the aircraft plane of symmetry and the horizontal plane, as shown in Fig. 1. A complete derivation of the equations of motion is presented in Ref. 16.

The reference equilibrium flight trajectory is on the envelope of a vertical cylinder, as shown in Fig. 2. It is determined by constant velocity and initial bank and glide angles.

The equilibrium gliding turn is obtained by solving Eqs. (1-8) with all time derivatives set to zero:

$$\dot{\alpha}=\dot{\beta}=\dot{p}=\dot{q}=\dot{r}=\dot{\theta}=\dot{\phi}=0 \quad (9)$$

This equilibrium is obtained by also assuming a coordinated turn; i.e., the resultant aerodynamic force lies in the plane of symmetry of the aircraft or, equivalently, the side force coefficient is equal to zero:

$$C_y=0 \quad (10)$$

The steady-state values of angle of attack ($\alpha$), sideslip angle ($\beta$), pitch attitude ($\theta$), the steady-state angular velocity ($p,q,r$) and three controls of the aircraft: elevator ($\delta_e$), rudder ($\delta_r$), and aileron ($\delta_a$) deflections, are computed by solving Eqs. (9) and (10), which present eight equations for the nine unknowns. An additional equation is obtained by realizing that $p,q,r$ are not really independent variables, but are determined by $\phi$, $\theta$, and the airplane turning rate $\dot{\psi}$.

These values of the respective state and control variables are used as initial conditions for integrating numerically the nonlinear equations of motion.

This digital simulation was carried out on an IBM (370/165) computer using CSMP language for a light, general aviation aircraft. Aircraft data and stability derivatives were computed by the methods described in Refs. 17 and 18 and are given in Appendix A.

## III. Qualitative Discussion

Simulation results show that the response of the aircraft to elevator input can be decomposed into three different motions taking place at almost separate time scales.

### A. Fast Longitudinal Motion (Short Period)

This motion (phase A) is very similar to the one experienced in symmetrical flight. During this phase, variations of the lateral variables are almost negligible. The elevator deflection produces a pitching moment which results in pitch rate, as can be seen from Eq. (4). Pitch rate generates a positive rate of change of angle of attack. This can be seen from Eq. (1), which can be written in simplified form:

$$\dot{\alpha}\simeq\Delta q-q_\infty S/(mV)C_{L_{\delta_e}}\Delta\delta_e>0 \quad (11)$$

The increase of pitch rate produces a rate of change in pitch attitude, as can be seen from Eq. (7). At this phase of the motion it is equal to

$$\dot{\theta}=\Delta q\cos\phi>0 \quad (12)$$

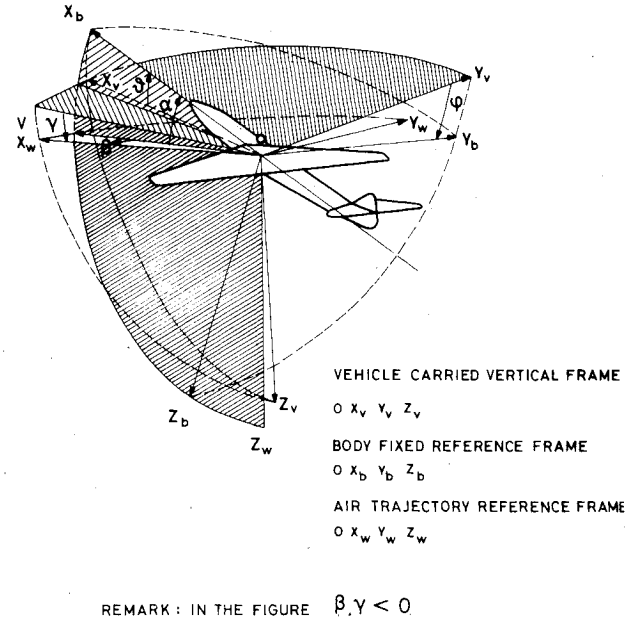


Fig. 1 Body, wind, and vehicle-carried vertical reference frames.

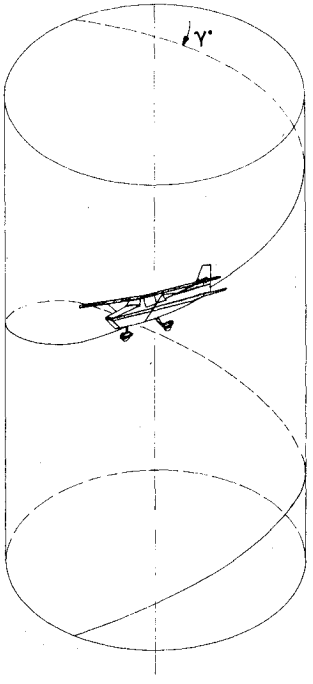

Fig. 2 Gliding turn flight path.

At the end of this short initial phase, *new equilibrium values* of angle of attack and pitch rate are reached.

### B. Divergent Lateral Motion

This motion (phase B) is induced by the rolling moment due to yaw rate. Since the stability derivative‡ $C_{l_r}$ is monotonically increasing with the lift coefficient (or equivalently with angle of attack), the increase of angle of attack experienced during the longitudinal fast motion increases the rolling moment which existed during the equilibrium gliding turn.

This phenomenon is the first one to create a cross-coupling between longitudinal and lateral dynamics of the aircraft. This cross-coupling can be characterized by a new stability derivative defined by

$$C_{l_\alpha} = (\partial C_{l_r}/\partial\alpha)_0 r_0 \tag{13}$$

The subscript *0* in Eq. (13) denotes the reference equilibrium condition the derivative was calculated for. As can be seen from Eq. (13), the stability derivative $C_{l_\alpha}$ is a function of the equilibrium yawing rate. Since the derivative $\partial C_{l_r}/\partial\alpha$ is positive, the derivative $C_{l_\alpha}$ has the same sign as $r_0$. Hence, for positive yawing rate, $C_{l_\alpha}$ is positive as well.

By using Eq. (13), the rolling moment Eq. (3) is rewritten in simplified form as

$$\dot{p} \simeq (q_\infty Sb/I_x) C_{l_\alpha} \Delta\alpha > 0 \qquad r_0 > 0 \tag{14}$$

Hence roll rate is developed owing to the increase of angle of attack. Roll rate combined with the increase of angle of attack causes an increase of sideslip angle. From Eq. (2) the rate of change of the sideslip angle is obtained by

$$\dot{\beta} \simeq p_0 \Delta\alpha + \alpha_0 \Delta p > 0 \tag{15}$$

The change of sideslip angle is followed by a change in yaw rate due to the directional stability of the aircraft. From Eq. (5),

$$\dot{r} \simeq (q_\infty Sb/I_z) C_{n_\beta} \Delta\beta > 0 \tag{16}$$

Once the yaw rate was increased, it generated additional roll rate since the rolling moment due to yaw rate is positive. The roll rate is followed by an increase of sideslip angle and then by a yaw rate which increases the roll rate again. This response in roll rate, sideslip angle, and yaw rate is known as the spiral divergence of the aircraft. Such phenomenon occurs if the "spiral stability coefficient" defined by

$$C_s \triangleq C_{l_\beta} C_{n_r} - C_{n_\beta} C_{l_r} \tag{17}$$

is negative as in most unswept, straight wing, general aviation aircraft.

### C. Combined Kinematic Response

This response is characterized by the interaction of bank, pitch, and flight-path angles. The roll rate experienced during the lateral spiral divergence phase increases the aircraft's bank angle. A good approximation for the change of bank angle is a pure integration of the roll rate

$$\dot{\phi} \simeq \Delta p > 0 \tag{18}$$

The combination of the increased bank angle and increasing yaw rate, developed during phase B, decreases the pitch attitude of the aircraft. The pitch attitude response of the aircraft in this phase is dominated by the yaw rate and bank angle changes, since the pitch rate had reached its equilibrium during phase A. The pitch attitude rate expression in Eq. (7) can now be approximated by

$$\Delta\dot{\theta} \simeq -(r_0 \cos\phi_0)\Delta\phi - \sin\phi_0 \Delta r < 0 \tag{19}$$

Hence the pitch attitude response during this phase is decreasing monotonically. The total response of the pitch attitude is a slight increase during phase A, and a monotonic decrease during the phases B and C, until finally it reaches a smaller equilibrium value than the one it had during the gliding turn.

The flight-path angle which is described by Eq. (8) can be approximated during this phase by the following equation:

$$\Delta\gamma \simeq \Delta\theta < 0 \tag{20}$$

This is due to the fact that during this phase the angle of attack is not changing any more and the sideslip angle is negligibly small. This implies that the flight-path angle response is similar to the response in pitch attitude, as described before. This leads to the following response of the aircraft for elevator deflection during a gliding turn: the initial response is a decrease in rate of descent, but very soon the rate of descent starts to increase, being accompanied by a tightened turn.

A block diagram showing the flow of events leading to the phenomenon is given in Fig. 3. Time history of the variables is depicted in Fig. 4 for a spiral dive developed as a consequence of a −5-deg elevator step input. The time history in Fig. 5 shows that for a different set of initial conditions the same elevator input results in a recovery from the glide.

## IV. Simulation Results

The simulation was performed for various initial equilibrium gliding turns characterized by speed, glide, and bank angles. Typical values for gliding turns were chosen. A systematic search for flight conditions for successful recovery from spiral dive by using elevator only was carried out. To obtain these flight conditions the following criterion for recovery by elevator only was defined.

Assuming an equilibrium flight trajectory $\gamma(t=0) < 0$ and elevator (only) step input $\Delta\delta_e$ such that

$$|\Delta\delta_e| < |\Delta\delta_e(\alpha_{\text{stall}})| \forall t \in [0, T]$$

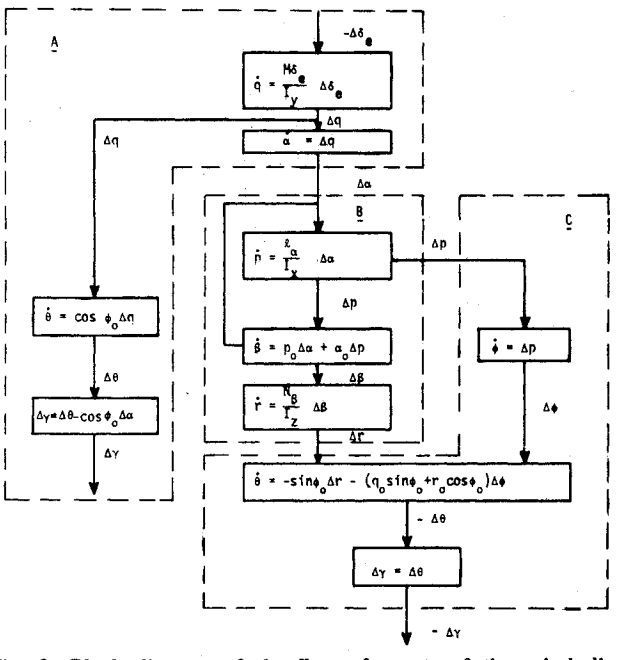


**Fig. 3 Block diagram of the flow of events of the spiral dive phenomenon.**

‡The stability derivatives are defined in Appendix B.

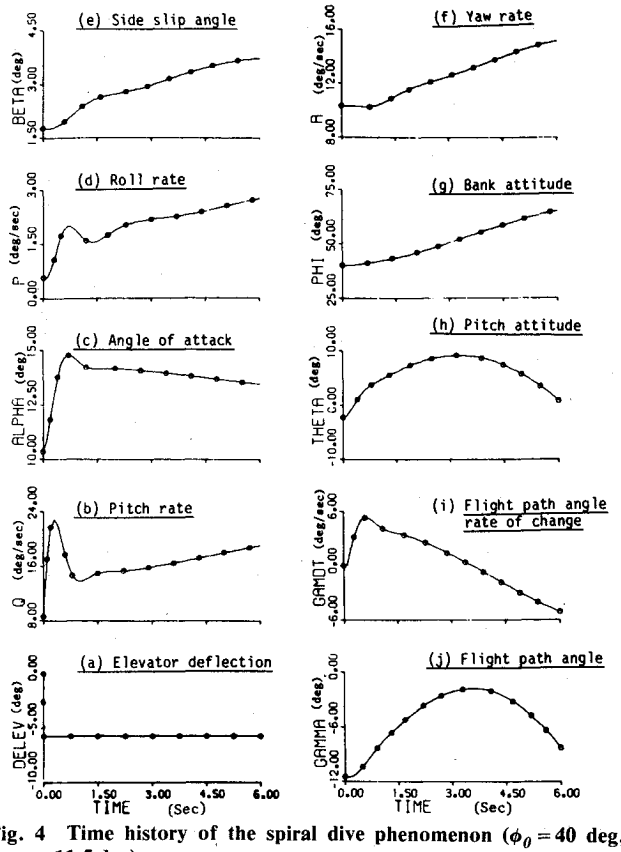


Fig. 4 Time history of the spiral dive phenomenon ($\phi_0 = 40$ deg, $\gamma_0 = -11.5$ deg).

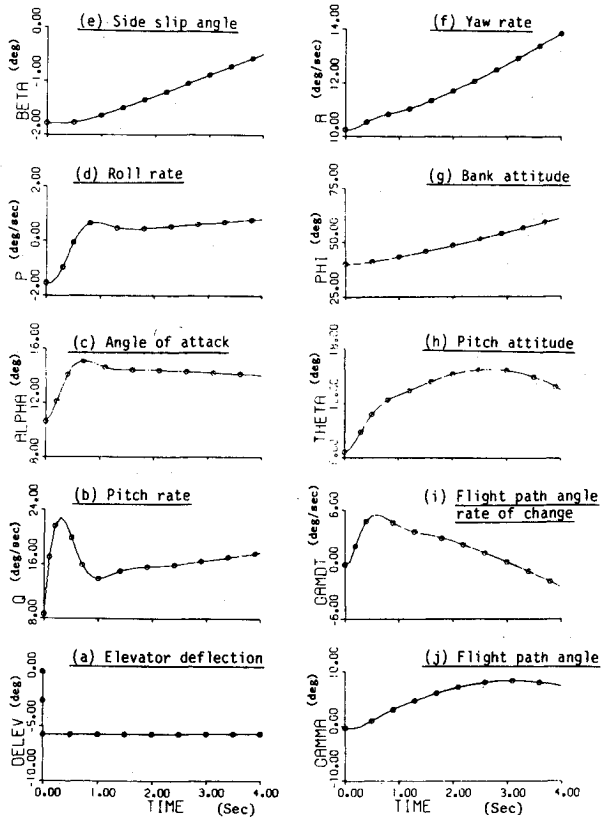


Fig. 5 Time history of a case of recovery ($\phi_0 = 40$ deg, $\gamma_0 = -0.5$ deg).

recovery is achieved if there exists some $t^* \in [0, T]$ such that

$$\operatorname{sign}\dot{\gamma}(t^*) = \operatorname{sign}\gamma(t^*) = +1 \tag{21}$$

The meaning of this criterion is that recovery is successful if descent can be stopped by using a maximum elevator deflection which does not cause the aircraft to stall.

From the simulation results it was found that recovery is unfavorable for steeper initial glide slopes, larger bank angles, and lower speeds. Figure 6 shows a map of bank and glide angles for a speed of 35 m/s. This map was drawn for a large number of simulations. A similar map is shown in Fig. 7 for two different velocities: 30 and 35 m/s.

For steeper initial glide slopes, recovery becomes more difficult since the time required to stop the descent becomes longer. By that time the spiral divergence is more developed, hence the lateral variables which affect the kinematic response of the aircraft become larger.

For larger bank angles the cross-coupling between longitudinal and lateral dynamics is stronger, hence the aircraft response is affected more by the divergent spiral motion.

Lower velocities or equivalently higher lift coefficients affect the recovery capability because, for the type of aircraft analyzed, the spiral stability coefficient becomes more negative at lower velocities and the rate of divergence of the spiral motion is higher.

## V. Description of the Spiral Dive Phenomenon with Linear Model

The equations of motion can be simplified by linearization about an equilibrium flight condition of the aircraft. Commonly such linearization is performed about trimmed straight and leveled flight and consequently separation between lateral and longitudinal dynamics equations is obtained. Since the spiral dive phenomenon occurs owing to the cross-coupling

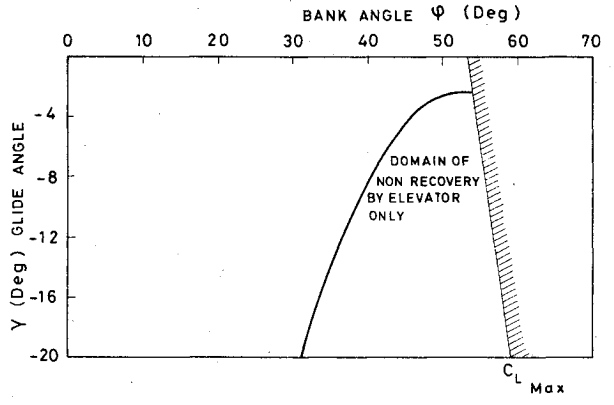


Fig. 6 Nonrecovery domain ($V = 35$ m/s).

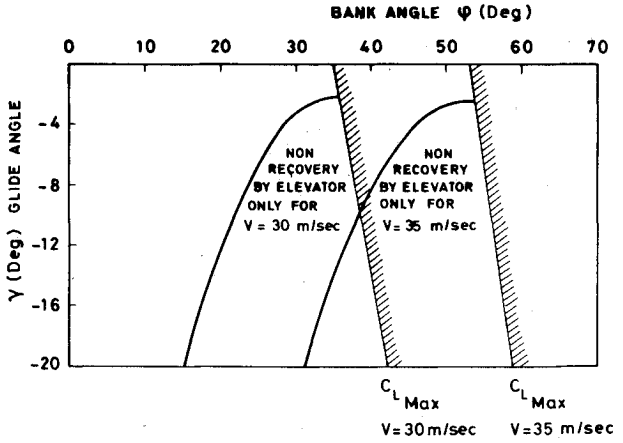


Fig. 7 Nonrecovery domain for different velocities.

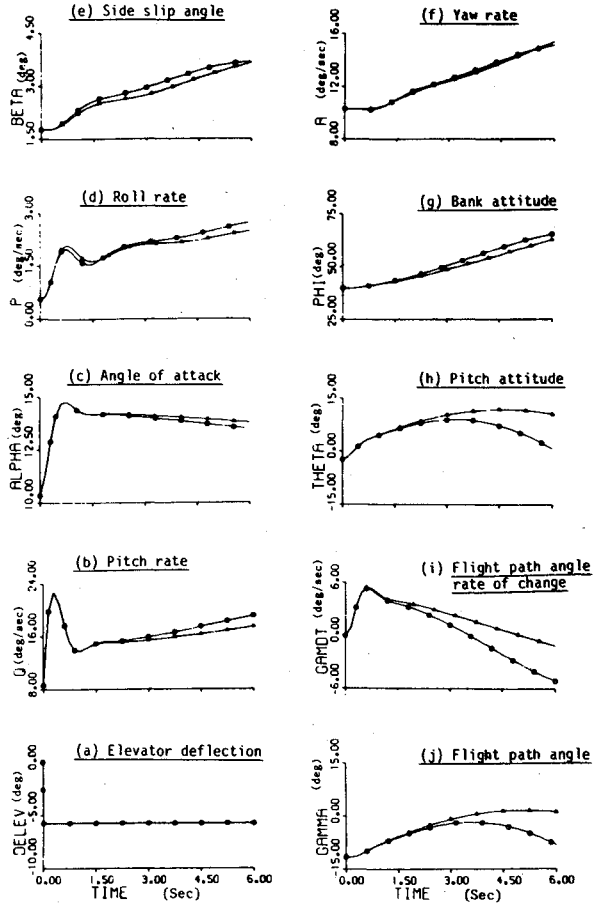


**Fig. 8 Time history of linearized equations of motion. Linearization point is equilibrium gliding turn [linear equations (Δ), nonlinear equations (○)].**

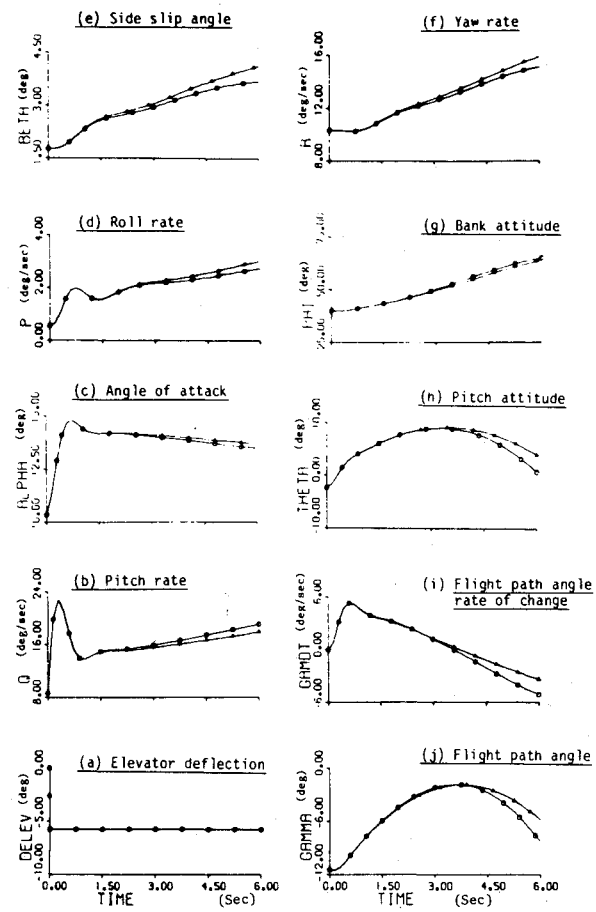


**Fig. 9 Time history of linearized equations of motion. Linearization point is longitudinal equilibrium [linear equations (Δ), nonlinear equations (○)].**

between longitudinal and lateral aircraft dynamics, it is obvious that such linearization is improper.

An appealing reference condition is the equilibrium gliding turn that was described at Sec. II. The linearization was performed using the method described by Adams.[19]

1) Linearization about the equilibrium gliding turn condition: The solution of the linearized equations of motion about the equilibrium gliding turn is shown in Fig. 8 compared to the nonlinear solution. It can be seen that the spiral dive phenomenon has not been obtained. The misadjustment between the two solutions is apparent in the roll rate time histories and it is due to the constant value taken for the stability derivative $C_{l_r}$ during the whole maneuver. This value is determined by the magnitude of the angle of attack at the start of the calculation, i.e., at the stabilized gliding turn condition. Thus the increase in angle of attack is not taken fully into account while calculating the roll rate.

2) Linearization about the new longitudinal equilibrium: The failure of the linearized model occurs because the large changes in the longitudinal state variables are not fully expressed. It was already found that the aircraft reaches an approximate equilibrium in the longitudinal state variables after a very short time, while the lateral state variables remain almost constant. A linearization was performed about this quasiequilibrium condition. The equations of motion were solved in two steps: a) The longitudinal equations of motion ($\alpha$, $q$) were solved while the lateral variables were kept constant. b) All the equations were solved, while using the values of $q$ and $\alpha$ obtained in step a for calculating the coefficients in the linearized equations.

The solution obtained by using this method follows with adequate accuracy the nonlinear solution, as is shown in Fig. 9.

## VI. Conclusions

This paper has presented results of a systematical investigation of the phenomenon known as spiral dive. The investigation was done by digital simulation of the aircraft response to elevator inputs during gliding turns. From the simulation it was found that the origin of this phenomenon is in the "cross-coupling" between longitudinal and lateral aircraft dynamics existing in all not entirely symmetrical flight conditions. The main cause for this cross-coupling is the rolling moment due to the yaw rate $C_{l_r}$ stability derivative which is increasing monotonically with angle of attack for the type of airplanes analyzed. A criterion for "recovery by elevator only" was stated and flight conditions for successful "recovery by elevator only" were determined. It was found that recovery becomes more difficult for steeper glide slopes, larger bank angles, and lower speeds.

An important conclusion of this investigation is that the inherent cross-coupling between longitudinal and lateral aircraft dynamics cannot be neglected even in the range of small angles of attack and very slow roll rates. Thus the convenient decoupling of longitudinal and lateral dynamics, frequently used in flight control design, may not be always justified.

## Appendix A: Aircraft Data and Stability Derivatives

$W = 1000$ kg
$S = 16.25$ m$^2$
$b = 11.2$ m
$\bar{c} = 1.5$ m

$I_x = 121.4$ kg-m-s$^2$
$I_y = 165.9$ kg-m-s$^2$
$I_z = 253.5$ kg-m-s$^2$

$C_{L_0} = 0.2$
$C_{L_\alpha} = 5.1$ rad$^{-1}$
$C_{L_{\delta_e}} = 0.688$ rad$^{-1}$

$C_{m_0} = 0.1$
$C_{m_\alpha} = -1.97$ rad$^{-1}$
$C_{m_{\delta_e}} = -1.72$ rad$^{-1}$

$C_{L_q} = 9.56\ \text{rad}^{-1}$ $\quad C_{m_q} = -16.3\ \text{rad}^{-1}$

$C_{y_\beta} = -0.337\ \text{rad}^{-1}$

$C_{y_{\delta_r}} = 0.097\ \text{rad}^{-1}$

$C_{n_\beta} = 0.057\ \text{rad}^{-1}$ $\quad C_{l_\beta} = -0.109\ \text{rad}^{-1}$

$C_{n_p} = (-0.018 - 0.03\alpha)\ \text{rad}^{-1}$ $\quad C_{l_p} = -0.48\ \text{rad}^{-1}$

$C_{n_r} = (-0.081 - 0.05\alpha)\ \text{rad}^{-1}$ $\quad C_{l_{\delta_r}} = 0.023\ \text{rad}^{-1}$

$C_{n_{\delta_r}} = -0.052\ \text{rad}^{-1}$ $\quad C_{l_{\delta_a}} = 0.092\ \text{rad}^{-1}$

$C_{n_{\delta_a}} = (-0.08\alpha)\ \text{rad}^{-1}$ $\quad C_{l_r} = (0.1 + 1.2\alpha)\ \text{rad}^{-1}$

## Appendix B: Stability Derivatives Definitions

$$C_{L_\alpha} = \frac{\partial C_L}{\partial \alpha} \qquad C_{m_\alpha} = \frac{\partial C_m}{\partial \alpha} \qquad C_{y_\beta} = \frac{\partial C_y}{\partial \beta}$$

$$C_{L_{\delta_e}} = \frac{\partial C_L}{\partial \delta_e} \qquad C_{m_{\delta_e}} = \frac{\partial C_m}{\partial \delta_e} \qquad C_{y_{\delta_r}} = \frac{\partial C_y}{\partial \delta_r}$$

$$C_{L_q} = \frac{\partial C_L}{\partial (q\bar{c}/2V)} \qquad C_{m_q} = \frac{\partial C_m}{\partial (q\bar{c}/2V)}$$

$$C_{l_\alpha} = \frac{\partial C_l}{\partial \alpha}$$

$$C_{n_\beta} = \frac{\partial C_n}{\partial \beta} \qquad C_{l_\beta} = \frac{\partial C_l}{\partial \beta}$$

$$C_{n_{\delta_r}} = \frac{\partial C_n}{\partial \delta_r} \qquad C_{l_{\delta_r}} = \frac{\partial C_l}{\partial \delta_r}$$

$$C_{n_{\delta_a}} = \frac{\partial C_n}{\partial \delta_a} \qquad C_{l_{\delta_a}} = \frac{\partial C_l}{\partial \delta_a}$$

$$C_{n_p} = \frac{\partial C_n}{\partial (pb/2V)} \qquad C_{l_p} = \frac{\partial C_l}{\partial (pb/2V)}$$

$$C_{n_r} = \frac{\partial C_n}{\partial (rb/2V)} \qquad C_{l_r} = \frac{\partial C_l}{\partial (rb/2V)}$$

## References


[1] "Jeppesen Private Pilot Course," Jeppesen Sanderson, Inc., Denver, Colo., 1979.

[2] Phillips, W.H., "Effect of Steady Rolling on Longitudinal and Directional Stability," NACA TN-1627, June 1948.

[3] Sternfield, L., "A Simplified Method for Approximating the Transient Motion in Angles of Attack and Sideslip During a Constant Rolling Maneuver," NACA Report 1344, 1958.

[4] Moul, M.T. and Brennan, T.R., "Approximate Method for Calculating Motions in Angles of Attack and Sideslip Due to Step Pitching and Yawing Moment Inputs During Steady Roll," NACA TN-4346, Sept. 1958.

[5] Rhoads, D.W. and Schuler, J.M., "A Theoretical and Experimental Study of Airplane Dynamics in Large Disturbance Maneuver," *Journal of the Aeronautical Sciences,* Vol. 24, July 1957, pp. 5-7, 526, 532.

[6] Hacker, T. and Oprisiu, C., "A Discussion of the Roll Coupling Problem," in *Progress in Aerospace Sciences,* Vol. 15, Pergamon Press, Oxford, 1974, pp. 151-180.

[7] Welch, J.D. and Wilson, R.E., "Cross-Coupling Dynamics and the Problem of Automatic Control in Rapid Rolls," *Journal of the Aeronautical Sciences,* Vol. 24, Oct. 1957, pp. 741-754.

[8] Haddad, E.K., "Study of Stability of Large Maneuvers of Airplanes," NASA CR-2447, 1974.

[9] Young, J.W., Schy, A.A., and Johnson, K.G., "Prediction of Jump Phenomena in Aircraft Maneuvers, Including Nonlinear Aerodynamic Effects," *Journal of Guidance and Control,* Vol. 1, Jan.-Feb. 1978, pp. 26-31.

[10] Mehra, R.K., Kessel, W.C., and Carroll, J.V., "Global Stability and Control Analysis of Aircraft High Angles of Attack," Report ONR-CR-215-248-1, Office of Naval Research, June 1977.

[11] Abzug, M.J., "Effect of Certain Steady Motions on Small Disturbance Airplane Motions," *Journal of the Aeronautical Sciences,* Vol. 21, Nov. 1954, pp. 749-762.

[12] Porter, R.F. and Loomis, J.P., "Examination of an Aerodynamic Coupling Phenomenon," *Journal of Aircraft,* Vol. 2, Nov.-Dec. 1965, pp. 553-556.

[13] Stengel, R.F., "Effect of Combined Roll Rate and Sideslip Angle on Aircraft Flight Stability," *Journal of Aircraft,* Vol. 12, Aug. 1975, pp. 683-685.

[14] Stengel, R.F., Taylor, J.H., Broussard, J.R., and Berry, P.W., "High Angle of Attack Stability and Control," Report ONR-CR215-237-1, Office of Naval Research, April 1976.

[15] Johnston, D.E. and Hogge, J.R., "Nonsymmetric Flight Influence on High-Angle of Attack Handling and Departure," *Journal of Aircraft,* Vol. 13, Feb. 1976, pp. 111-118.

[16] Etkin, B., *Dynamics of Atmospheric Flight,* Wiley, New York, 1972.

[17] Wolowicz, C.H. and Yancey, R.B., "Longitudinal Aerodynamic Characteristics of Light, Twin Engine, Propeller Driven Airplanes," NASA TN D-6800, June 1972.

[18] Wolowicz, C.H. and Yancey, R.B., "Lateral Directional Aerodynamic Characteristics of Light, Twin Engine, Propeller Driven Airplanes," NASA TN D-6946, Oct. 1972.

[19] Adams, W.A., "Analytic Prediction of Airplane Equilibrium Spin Characteristics," NASA TN D-6926, Nov. 1972.